agronomy

MDPI

Article

Saturated Hydraulic Conductivity of Nine Soils According to Water Quality, Soil Texture, and Clay Mineralogy

Clarissa Buarque Vieira [1,*], Gabriel Henrique Maximo Clarindo Silva [1], Brivaldo Gomes de Almeida [1], Luiz Guilherme Medeiros Pessoa [2], Fernando José Freire [1], Valdomiro Severino de Souza Junior [1], Hidelblandi Farias de Melo [3], Luara Gabriella Gomes de Lima [1], Rodrigo Francisco do Nascimento Paiva [1], Jorge Freire da Silva Ferreira [4,*] and Maria Betânia Galvão dos Santos Freire [1]

[1] Agronomy Department, Federal Rural University of Pernambuco, Recife 52171-900, Pernambuco, Brazil; gabriagro@hotmail.com (G.H.M.C.S.); brivaldo.almeida@ufrpe.br (B.G.d.A.); fernando.freire@ufrpe.br (F.J.F.); valdomiro.souzajunior@ufrpe.br (V.S.d.S.J.); luara_gomees@hotmail.com (L.G.G.d.L.); rodrigofrancisco.n44@gmail.com (R.F.d.N.P.); maria.freire@ufrpe.br (M.B.G.d.S.F.)
[2] Graduate Program in Crop Production, Federal Rural University of Pernambuco, Serra Talhada 56909-535, Pernambuco, Brazil; luiz.pessoa@ufrpe.br
[3] Soil Department, Federal University of Viçosa, Viçosa 36570-900, Minas Gerais, Brazil; hidelblandi@ufv.br
[4] US Salinity Laboratory (USDA-ARS), Riverside, CA 92507, USA
* Correspondence: clarissa.buarque@ufrpe.br (C.B.V.); jorge.ferreira@usda.gov (J.F.d.S.F.)

Abstract: Water quality affects soils by promoting their degradation by the accumulation of salts that will lead to salinization and sodification. However, the magnitude of these processes varies with soil attributes. Saturated hydraulic conductivity (K_{sat}) is the rate at which water passes through saturated soil, which is fundamental to determining water movement through the soil profile. The K_{sat} may differ from soil to soil according to the sodium adsorption ratio (SAR), water electrical conductivity (EC_w), soil texture, and clay mineralogical assemblage. In this study, an experiment with vertical columns and constant-load permeameters was conducted to evaluate changes in soil K_{sat} with waters comprising five EC_w values (128, 718, 1709, 2865, and 4671 μS cm^{-1}) and five SAR values [0, 5, 12, 20, and 30 (mmol$_c$ L^{-1})$^{0.5}$] in combination. Horizons from nine northeastern Brazilian soils (ranging from tropical to semiarid) were selected according to their texture and clay mineralogical composition. The data obtained were fit with multiple regression equations for K_{sat} as a function of EC_w and SAR. This study also determined the null SAR at each EC_w level, using K_{sat} = 0 on each equation, to predict the SAR needed to achieve zero drainage on each soil for each EC_w level and the threshold electrolyte concentration (C_{TH}) that would lead to a 20% reduction of maximum K_{sat}. Neither the EC_w nor SAR of the applied waters affected the K_{sat} of soils with a mineralogical assemblage of oxides and kaolinite such as Ferralsol, Nitisol, and Lixisol, with an average K_{sat} of 2.75, 6.06, and 3.33 cm h^{-1}, respectively. In smectite- and illite-rich soils, the K_{sat} increased with higher EC_w levels and decreased with higher SAR levels, especially comparing the soil's estimated K_{sat} for water with low EC_w and high SAR in combination (EC_w of 128 μS cm^{-1} and SAR 30) and water with high EC_w and low SAR in combination (EC_w of 4671 μS cm^{-1} and SAR 0) such as Regosol (4.95 to 10.94 cm h^{-1}); Vertisol (0.28 to 2.04 cm h^{-1}); Planosol (0 to 0.29 cm h^{-1}); Luvisol (0.46 to 2.12 cm h^{-1}); Cambisol (0 to 0.23 cm h^{-1}); and Fluvisol (1.87 to 3.34 cm h^{-1}). The C_{TH} was easily reached in soils with high concentrations of highly active clays such as smectites. In sandy soils, the target C_{TH} was only reached under extremely high SAR values, indicating a greater resistance of these soils to salinization/sodification. Due to their mineralogical assemblage, soils from tropical sub-humid/hot and semiarid climates were more affected by treatments than soils from tropical humid/hot climates, indicating serious risks of physical and chemical degradation. The results showed the importance of monitoring water quality for irrigation, mainly in less weathered, more clayey soils,

Academic Editor: Eduardo Guimarães Couto

Received: 19 February 2025
Revised: 25 March 2025
Accepted: 28 March 2025
Published: 30 March 2025

Citation: Vieira, C.B.; Silva, G.H.M.C.; Almeida, B.G.d.; Pessoa, L.G.M.; Freire, F.J.; de Souza Junior, V.S.; Melo, H.F.d.; Lima, L.G.G.d.; Paiva, R.F.d.N.; Ferreira, J.F.d.S.; et al. Saturated Hydraulic Conductivity of Nine Soils According to Water Quality, Soil Texture, and Clay Mineralogy. *Agronomy* **2025**, *15*, 864. https://doi.org/10.3390/agronomy15040864

with high clay activity to minimize the rate of salt accumulation in soils of the Brazilian semiarid region. Our study also proved that clay mineralogy had more influence on the K_{sat} than clay concentration, mainly in soils irrigated with saline and sodic waters, and that soils with highly active smectite are more prone to degradation than soils with high concentrations of kaolinite.

Keywords: salinity; sodicity; threshold electrolyte concentration; granulometric composition; mineralogical assemblage

1. Introduction

Irrigation water with high concentrations of salts and sodium, without proper management, can aggravate soil salinization and/or sodification, depending on the soil's composition and environmental conditions [1,2]. In arid and semiarid regions, irrigation with poor-quality water is common due to freshwater scarcity [3]. Thus, measuring the impact of irrigation waters on soil properties has become a key factor in assessing their use in irrigated systems [1]. On the other hand, the excessive use of irrigation water without efficient drainage has caused the accumulation of salts and waterlogging in some soil profiles [4].

As a physical property, the soil saturated hydraulic conductivity (K_{sat}) is directly related to water movement in the soil and the consequent maintenance of biological life in the environment [5,6]. Natural and anthropic factors, such as densification, compaction, soil amendment application, salt concentration, and different types of tillage systems can affect soil hydraulic conductivity [7]. Thus, K_{sat} depends on aggregation, total porosity, pore size, flocculation, organic matter, soil salinity, and soil texture [6]. Soil natural hydraulic conductivity is obtained when the soil is saturated and has a constant infiltration rate [8].

Saturated hydraulic conductivity is strongly related to the electrolyte concentration and the balance between monovalent and divalent ions [9]. In most soils, the knowledge of the threshold electrolyte concentration (C_{TH}), which is reached when the soil's K_{sat} is reduced by 20% [1], is essential for their proper management under different clay concentration and types. This knowledge enables detecting risks of soil salinization and sodification and can be used in studies for the recovery of degraded areas.

The dynamics and the effects of salts in the soils (in low or high concentration) are associated with the chemical, physical, and mineralogical properties of each soil and the chemical properties of the irrigation water [10,11]. Thus, proper soil management requires techniques that prevent its degradation and the consequent abandonment of the land.

Tropical soils, such as Brazilian soils, are mostly highly weathered and clayey, with the clay mineralogical assemblage being rich in oxides and kaolinite [12]. Based on this, 60% of Brazilian soils are predominately Ferralsols and Lixisols [12]. Besides that, part of Brazilian territory is influenced by an arid and semiarid climate [13,14] with less weathered soils, rich in smectite, illite, and kaolinite, such as Vertisols, Planosols, Regosols, Cambisols, Fluvisols, and Luvisols [15,16].

Soils from arid and semiarid regions are usually undergoing degradation due to salt and sodium accumulation, where waters with poor chemical quality, applied through irrigation, affect their agricultural sustainability [17]. Nevertheless, studies that investigate the effects of using distinct water qualities on the soil structure are still scarce, especially in Brazilian soils.

Thus, the objective of this study was to investigate changes in the K_{sat} on soils from tropical and semiarid regions of Brazil, with different texture and mineralogical assem-

blages, under irrigation water with increasing levels of salinity and sodicity. Consequently, the object was to answer the following question: How to properly manager irrigation waters with a different electrolyte concentration (EC_w) and sodium adsorption rate (SAR) in soils with a distinct texture and mineralogical composition without degrading them?

This study evaluated the K_{sat} of nine different soil types under laboratory conditions with an application of 25 percolating waters with increasing concentrations of salts, expressed by electrical conductivity (EC_w) and Na^+ proportions (SAR). The analyses showed the changes in K_{sat} and in threshold electrolyte concentration when Brazilian soils with distinct texture and mineralogy were treated with water featuring different chemical qualities. These data will enable us to estimate the susceptibility of soils to degradation under irrigation with different types of water.

2. Material and Methods

2.1. Soil Sampling and Characterization

For this study, soil samples were collected according to previous classified soils from Pernambuco state, Northeast Brazil. The selected soils were as follows: Umbric Ferralsol; Ferralic Nitisol; Haplic Lixisol; Eutric Regosol; Pellic Vertisol; Albic Planosol; Chromic Luvisol; Fluvic Cambisol; and Eutric Fluvisol [18–25]. The soils were selected based on the climate zones (tropical humid/hot, tropical sub-humid, and semiarid climates), texture (soils from sandy to clayey), and mineralogical assemblage of the clay fraction (soils with a constitution of 1:1 minerals such as kaolinite; soils with 2:1 minerals such as smectites and illites; and soils with low and high concentration of Fe (hydr)oxides) as described in Figure 1 and Tables 1 and 4.

Figure 1 shows the spatial distribution of the soil sampling points, according to three different physiographic zones and climates (A = Am; B = As; C = Bsh).

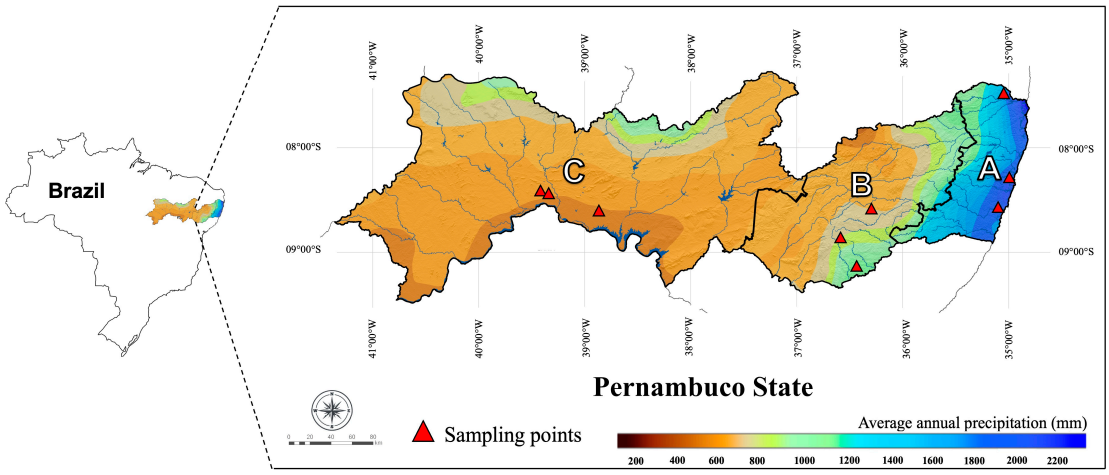

Figure 1. Soil sampling points in Pernambuco, Northeastern Brazil. (A) Rain forest zone—tropical humid/hot climate; (B) intermediary zone—tropical sub-humid/hot climate; and (C) inland zone—semiarid climate. Adapted from Governo do Estado de Pernambuco [26].

The samples were air-dried, crushed, and sieved through a 2 mm mesh for soil characterization. Soil samples of preserved structures were also collected for physical analyses in volumetric cylinders with 100 cm^3.

Table 1. Soils classification by IUSS Working Group WRB [27], depth of the sampling horizons, climate, and soils spatial localization.

Soil Classification WRB	Depth [1] (cm)	Climate	Geographic Coordinates
Umbric Ferralsol	155–200	Tropical—humid/hot	7°25′23.2″ S 35°10′51.5″ W
Ferralic Nitisol	50–90	Tropical—humid/hot	8°35′30″ S 35°6′59″ W
Haplic Lixisol	50–70	Tropical—humid/hot	8°18′′0″ S 35°01′26″ W
Eutric Regosol	0–20	Tropical—sub-humid/hot	8°29′50″ S 36°14′28″ W
Pellic Vertisol	20–68	Tropical—sub-humid/hot	08°29′53″ S 36°14′25″ W
Albic Planosol	80–110	Tropical—sub-humid/hot	9°8′29.8″ S 36°28′38,8″ W
Chromic Luvisol	20–40	Semiarid	8°44′26.1″ S 38°51′29.9″ W
Fluvic Cambisol	26–66	Semiarid	8°30′45″ S 39°22′59″ W
Eutric Fluvisol	0–20	Semiarid	8°30′56″ S 39°23′06″ W

[1] Depth of the diagnostic horizon for each soil.

The evaluated chemical properties were as follows: pH (1:2.5 water and KCl 1 mol L^{-1}); soil electrical conductivity (EC_e) by the saturated paste extract method and soluble cations (Ca^{2+}, Mg^{2+}, Na^+, and K^+) by the saturated paste extract method; exchangeable cations (Ca^{2+}, Mg^{2+}, Na^+, and K^+) extracted by the ammonium acetate (1 mol L^{-1}) method; cation exchange capacity (CEC) assessed by the index cation method; exchangeable aluminum extracted by KCl 1 mol L^{-1}; potential acidity (H + Al) extracted by calcium acetate (1 mol L^{-1}); and total organic carbon (TOC) determined with potassium dichromate [28] (Tables 2 and 3). Ca^{2+} and Mg^{2+} were measured by atomic absorption spectrophotometry, and Na^+ and K^+ were measured by flame photometry. These adopted methods are described by Teixeira et al. [29] and Richards [30]. The base saturation (BS), exchangeable sodium percentage (ESP), sodium adsorption ratio (SAR), aluminum saturation (AlS), and clay activity index (AI) were also calculated.

Table 2. Chemical characterization of soils: electrical conductivity (EC_e), soluble cations, and sodium adsorption ratio (SAR) by the saturated paste extract method.

Soil	EC_e dS m^{-1}	Soluble Cations				SAR $(mmol_c\ L^{-1})^{0.5}$
		Ca^{2+}	Mg^{2+}	Na^+	K^+	
		$mmol_c\ L^{-1}$				
Umbric Ferralsol	0.25	0.37	0.67	1.46	0.04	2.02
Ferralic Nitisol	0.22	0.26	0.28	1.01	0.08	1.93
Haplic Lixisol	0.17	0.30	0.09	0.94	0.05	2.14
Eutric Regosol	0.42	0.73	0.34	0.92	0.40	1.26
Pellic Vertisol	1.00	1.23	1.83	6.71	0.12	5.42
Albic Planosol	3.72	2.77	5.28	33.43	0.27	16.66
Chromic Luvisol	0.67	2.38	1.85	3.21	0.03	2.21
Fluvic Cambisol	22.35	70.89	62.21	196.20	0.25	24.05
Eutric Fluvisol	2.79	17.09	5.08	2.10	3.04	0.63

Table 3. Chemical characterization of soils: pH, delta pH (ΔpH), exchangeable cations, potential acidity, cation exchange capacity (CEC), base saturation (BS), aluminum saturation (AlS), exchangeable sodium percentage (ESP), clay activity index (AI), and total organic carbon (TOC).

Soil	pH		ΔpH [2]	Ca^{2+}	Mg^{2+}	Na^{+}	K^{+}	Al^{3+}	H+Al	CEC	AI	BS	AlS	ESP	TOC
	Water [1]	KCl					$cmol_c\ kg^{-1}$						%		$g\ kg^{-1}$
Umbric Ferralsol	4.65	4.00	−0.65	1.15	0.52	0.07	0.07	1.46	4.50	6.31	8.82	28.68	44.64	1.09	4.45
Ferralic Nitisol	4.73	3.95	−0.78	2.00	0.46	0.04	0.12	4.99	8.79	11.41	23.69	22.96	65.57	0.34	6.15
Haplic Lixisol	4.83	3.87	−0.96	0.58	0.32	0.13	0.18	12.02	16.30	17.50	35.23	6.91	90.85	0.80	7.83
Eutric Regosol	5.82	5.05	−0.77	1.22	0.35	0.00	0.10	0.00	0.72	2.39	N/A [3]	69.87	0.00	0.00	5.39
Pellic Vertisol	8.78	6.49	−2.28	18.08	12.42	1.12	0.44	0.00	0.00	32.06	75.44	100	0.00	3.48	5.09
Albic Planosol	6.79	5.14	−1.65	5.55	8.86	2.21	0.47	0.00	1.12	18.21	43.71	93.85	0.00	12.15	2.63
Chromic Luvisol	7.00	5.56	−1.44	10.46	6.70	0.18	0.20	0.00	1.06	18.60	61.75	94.30	0.00	0.97	5.28
Fluvic Cambisol	6.07	5.53	−0.53	5.08	2.82	1.33	0.14	0.00	0.60	9.97	43.19	93.98	0.00	13.31	2.58
Eutric Fluvisol	7.39	6.99	−0.40	8.82	1.79	0.05	0.84	0.00	0.43	11.93	N/A [3]	96.40	0.00	0.42	16.23

[1] pH in water (1:2.5); [2] $\Delta pH = pH_{KCl} - pH_{water}$. [3] Not Applicable due to their sand concentration.

Table 4. Soil physical characterization: granulometric fractions (sand, silt, and clay), flocculation index (FI), soil bulk density (SBD), soil particle density (SPD), and total porosity (TP).

Soil	Sand		Silt	Clay	FI	SBD	SPD	TP	Texture	Mineralogical Assembly [1]
	Coarse	Fine								
	$g\ kg^{-1}$				%	$g\ cm^{-3}$		%		
Umbric Ferralsol	124.40	67.78	92.21	715.60	100	1.45	2.68	52.30	Clay	K, Gh
Ferralic Nitisol	247.01	89.60	162.73	481.53	100	1.33	2.85	56.37	Clay	K, Hm, Gh
Haplic Lixisol	191.24	110.04	202.95	496.68	100	1.32	2.75	59.10	Clay	HIS, K, Gh
Eutric Regosol	697.72	179.12	94.94	28.22	29	1.67	2.76	ND [2]	Loamy Clay	I, K, Fd
Pellic Vertisol	181.35	127.76	266.13	424.98	95	1.65	2.69	ND [2]	Clay	S, Tc
Albic Planosol	365.67	127.76	89.98	416.59	22	1.71	2.68	43.20	Clay	S, I, K
Chromic Luvisol	278.50	293.00	127.26	301.23	63	1.95	2.87	45.97	Sandy Clay Loam	S, I, K, Gh, Hm
Fluvic Cambisol	73.53	348.41	347.24	230.82	93	1.67	2.71	41.22	Loam	S, I, K
Eutric Fluvisol	50.15	531.10	298.77	119.97	68	1.31	2.55	56.39	Sandy Loam	S, I, K

[1] K: kaolinite; S: smectite; I: illite; HIS: smectite with hydroxy-aluminum interlayer; Hm: hematite; Gh: goethite; Fd: feldspar; Tc: talc. [2] Not determined.

The evaluated physical properties were soil granulometric composition and water-dispersible clay (WDC) [31]; soil bulk density (SBD) as assessed by the volumetric ring method [32]; particle density (SPD) as assessed by the volumetric flask method [33]; and total porosity (TP) as assessed saturation with water for 24 h and drying at 105 °C of the unmixed soil of the volumetric ring. The flocculation index was calculated using total clay and water-dispersible clay FI = (Clay − CDW)/Clayx100 [31] (Table 4).

The sandy texture in the Eutric Regosol did not allow for the collection of volumetric rings, requiring that the assembling of the cylinders be realized in the laboratory to determine the bulk density. The volumetric ring also could not be collected for Pellic Vertisol

due to the presence of deep and wide cracks; thus, bulk density analysis was carried out by the clod method [34].

For mineralogical characterization of the clay fraction, crystalline and amorphous iron oxides were determined (Table 5), extracted with dithionite–citrate–bicarbonate and sodium oxalate solutions, respectively. Fe concentration was measured by atomic absorption spectrophotometry [35]. Mineralogical analysis of the clay fraction by x-ray diffraction was also carried out with the necessary treatments to identify 1:1 clay, 2:1 clay, and oxides (Table 4).

Table 5. Values of free iron oxides extracted with sodium dithionite–citrate–bicarbonate (Fed), amorphous iron extracted with sodium oxalate (Feo), and the relationship between free and amorphous iron oxides.

Soil	Horizon	Fed	Feo	Feo/Fed
		g kg^{-1}		
Umbric Ferralsol	Bw	26.69	0.36	0.01
Ferralic Nitisol	Bt1	122.77	2.46	0.02
Haplic Lixisol	Bt	8.40	2.79	0.33
Eutric Regosol	A	0.83	0.24	0.29
Pellic Vertisol	Biv	6.14	1.36	0.22
Albic Planosol	Btg	10.76	1.18	0.11
Chromic Luvisol	Btvnz	25.22	1.76	0.07
Fluvic Cambisol	Binz1	20.56	2.24	0.11
Eutric Fluvisol	Ap	7.44	1.37	0.18

To identify and characterize the minerals in the clay fraction, treatments of saturation by K and Mg were carried out. For samples saturated with K (KCl 1 mol L^{-1}), successive heating treatments were performed (25, 110, 350, and 550 °C). Samples saturated with Mg ($MgCl_2$ 1 mol L^{-1}) were later solvated with glycerol to evaluate the expansion of the minerals [36]. Finally, minerals in the clay fraction were identified by interplanar spacing (d) and by the trend of the diffraction peaks, according to saturation (K and Mg) and thermal treatments (Supplementary Figure S1) [36–38].

2.2. Saturated Hydraulic Conductivity Experiment

The experiment was conducted at the Federal Rural University of Pernambuco, Recife—PE, Brazil, from April 2019 to December 2019. It was carried out in a 5 × 5 factorial arrangement (5 EC values and 5 SAR values in percolating waters) across 9 soils, in randomized blocks, with four replicates, totaling 100 experimental units for each soil and 900 percolation stations (25 percolating waters × 4 replicates × 9 soils = 900 experimental units). In each soil, 25 saline solutions (percolating solutions) were applied, with an EC_w of 128, 718, 1709, 2865, and 4671 µS cm^{-1} and SAR of 0, 5, 12, 20, and 30 (mmol$_c$ L^{-1})$^{0.5}$.

To build the waters for the percolation assay, we calculated the proportions of NaCl and $CaCl_2$ to achieve target EC_w values of 100, 600, 1500, 2500, and 4000 µS cm^{-1}. Then, the real EC_w of each water sample was measured using an electrical conductivity meter, resulting in average EC_w values of 128, 718, 1709, 2865, and 4671 µS cm^{-1}. The EC_w and SAR levels were selected based on a previous study [39] and Richards' study [30], that considers water salinities from "low" to "very-high" salinity (EC_w of 100 to 5000 µS cm^{-1}) and "low" to "very-high" sodicity (SAR of 0 to 30). According to Richards [30], saline waters range from C1 (low-salinity water) to C4 (very-high salinity water) and sodic waters range from S1 (low-sodicity water) to S4 (very-high sodicity water). So, our study simulated percolating waters from C1S1 to C4S4 with 25 types of water (with varying EC_w and SAR). These treatments represent waters found in tropical agricultural regions (non-saline/non-

sodic), as in the Amazon region, to the arid and semiarid climates (saline and/or sodic) found in Brazil.

For the experiment, columns were prepared in PVC tubes measuring 5 cm in diameter and 15 cm in height. The soil was added until it reached 5 cm in height in the PVC tubes (100 cm^3 of soil samples). Inside the columns, the characteristic bulk density for each soil was achieved by adding three layers of 1.7 cm (each) totaling 5 cm of soil. Afterward, saturating solutions were used to adjust the Na:Ca ratio to establish the SAR of each treatment, with saturation corresponding to 2/3 of the height of the soil sample for 48 h. The solutions were prepared to reach a final concentration of 50 $mmol_c\ L^{-1}$, with NaCl and $CaCl_2$ salts, at the established SAR [0, 5, 12, 20, and 30 $(mmol_c\ L^{-1})^{0.5}$], according to Klute [40] and Freire et al. [39].

After saturation with solutions that regulated only the SAR in each soil, vertical column and constant load permeameters were installed to apply percolating solutions at different EC_w levels (maintaining the initial SAR) until reaching the balance between the EC_w of the percolating and leached solutions. The EC_w of each percolating solution was measured throughout the experiment, and the values used in the mathematical adjustments of the K_{sat} at the end of the experiment corresponded to the average EC_w for each solution.

Subsequently, soil columns were kept in containers with the final solutions (EC_w and SAR of each treatment) for 24 h. After completing the adjustment of EC_w and SAR, permeameters were reassembled to determine the K_{sat}. The final solutions were applied to the columns using the Mariotte bottle system to keep the constant load (Figure 2).

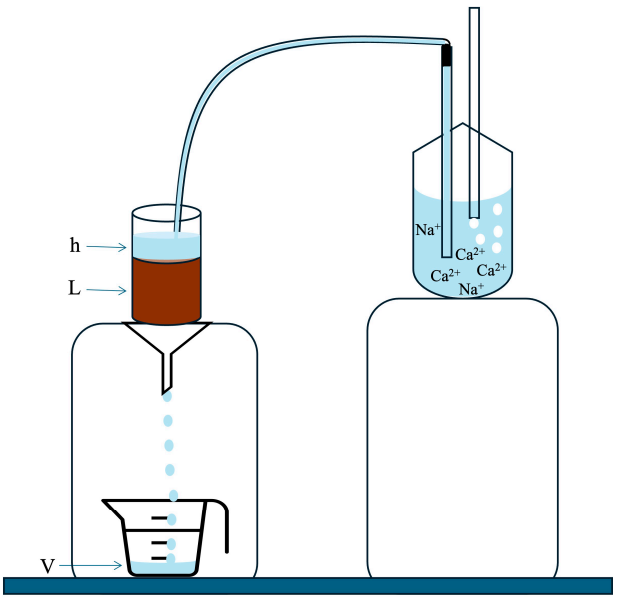

Figure 2. Mariotte bottle system used to determine water percolation rates through different water-saturated soils when using waters of different electrical conductivity, sodium adsorption ratio (SAR), and ionic composition, according to the experimental design. V = percolated volume (cm^3); L = soil sample thickness (cm); h = hydraulic load (cm).

The K_{sat} was determined in the columns after the passage of percolating solutions in laboratory conditions. Percolated volumes per unit of time were recorded at least three times, after equilibrium. K_{sat} was calculated following the equation below:

$$K_{sat} = \frac{V.L}{A.t.(h + L)}$$

where K_{sat} is the saturated hydraulic conductivity (cm h^{-1}); V is the percolated volume (cm^3); L is the soil sample thickness (cm); A is the transverse sectional area of the soil column (cm^2); t is the time; and h is the hydraulic load (cm).

2.3. Statistical Analysis

The K_{sat} data were subjected to the Shapiro–Wilk normality test and Levene homoscedasticity test. Then, an analysis of variance (ANOVA) was performed. Thus, having verified the significance of the interactions of the quantitative factors (EC_w and SAR) with the soils, multiple regression was chosen with the EC_w and SAR variables within each soil type, obtaining three-dimensional surfaces for each soil, as well as cuts that were made in these surfaces, to evaluate the trend of EC_w in relation to SAR. The selection of the best regression model that explained the trend of the data was performed by applying the *t*-test ($p < 0.10$) to the model parameters, selecting the model with the highest and most significant coefficients.

ANOVA was also used to verify whether there was a significant interaction between the EC_w and SAR factors for the K_{sat} data, that is, to show that these variables are not correlated.

Threshold electrolyte concentrations (C_{TH}) were calculated based on the 20% decrease from the maximum K_{sat}, using the mathematical models established by this study. We also calculated the electrolytic concentration that would lead to zero hydraulic conductivity (null K_{sat}) for the evaluated soils (equating the equation to $K_{sat} = 0$ in each EC_w value), indicating irrigation problems in situations of different EC_w and SAR values for the waters.

3. Results

3.1. Saturated Hydraulic Conductivity

Figure 3 shows the saturated hydraulic conductivity (K_{sat}) of the nine soils evaluated as a function of the EC_w and SAR of each percolating water. The K_{sat} data generated three-dimensional surfaces that allow for the visualization of the hydraulic conductivity trend of each soil after the increase in the EC_w and SAR (Figure 3). The K_{sat} varied among the soils, ranging from moderately fast to very slow, depending on the particle size and mineralogy of each soil.

The K_{sat} of highly weathered soils (Umbric Ferralsol, Ferralic Nitisol, and Haplic Lixisol) had no significant differences due to any combination of EC_w and SAR of percolating waters up to the limits tested in this study. On the other hand, the quality of the waters applied significantly changed the K_{sat} in less weathered soils, such as Eutric Regosol, Pellic Vertisol, Chromic Luvisol, Eutric Fluvisol, Fluvic Cambisol, and Albic Planosol, with a decrease in hydraulic conductivity triggered by a low EC_w and/or high SAR (Figure 3). These soils showed K_{sat} variations for the different tested waters with the adjustment of multiple regression equations of hydraulic conductivity depending on the EC_w and SAR of the tested waters (Table 6).

We also evaluated the effect of the SAR on each EC_w value (cuts in the three-dimensional surfaces) of the waters based on the equations applied for each of the six soils with significant differences in the K_{sat} (Figure 4). For all six soils, the increase in the SAR caused a decrease in the K_{sat}, and this trend was more significant at low EC_w values, corroborating the results presented by the three-dimensional surfaces (Figure 3).

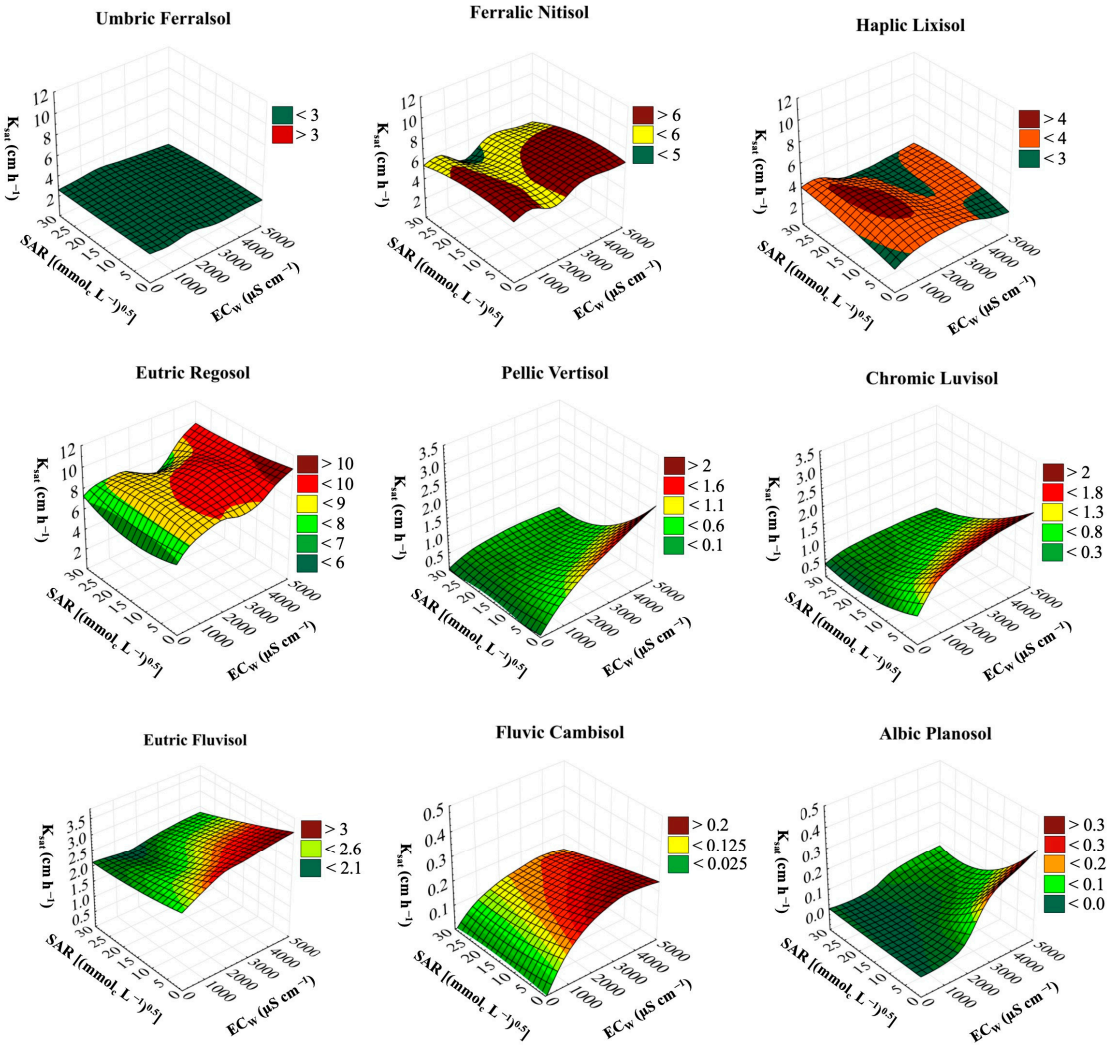

Figure 3. Three-dimensional surfaces of the saturated hydraulic conductivity (K_{sat}) for the soils studied, based on the EC_w and SAR of each percolating water.

Table 6. Multiple regression equations for saturated hydraulic conductivity as a function of the electrical conductivity (EC_w in µS cm^{-1}) and sodium adsorption ratio (SAR) of percolating solutions.

Soil	Equation	R^2	CV [1]
Umbric Ferralsol	$\overline{K}_{sat}$ = 2.7459	-	25.03
Ferralic Nitisol	$\overline{K}_{sat}$ = 6.0558	-	29.20
Haplic Lixisol	$\overline{K}_{sat}$ = 3.3313	-	15.98[2]
Eutric Regosol	$\overline{K}_{sat}$ = 6.03167 + 0.0017991 ** EC − 0.000000160069EC $^{2,\circ}$ − 0.0435899SAR **	0.7209	20.61
Pellic Vertisol	$\overline{K}_{sat}$ = 0.372869 + 0.000358036 *** EC − 0.0487104 *** SAR + 0.00152272 *** SAR ^{2} − 0.0000114532 *** EC SAR	0.9231	11.76[2]
Albic Planosol	$\overline{K}_{sat}$ = −0.0181408 + 0.0000662413 *** CE – 0.00561443 $^\circ$ RAS + 0.000229691 * RAS ^{2} – 0.00000204295 *** EC SAR	0.7815	4.50[2]
Chromic Luvisol	$\overline{K}_{sat}$ = 0.969163 + 0.000571572 *** EC − 0.0000000694489 ** EC ^{2} − 0.0609834 *** SAR + 0.0014585 *** SAR ^{2} − 0.000017605 * CE SAR + 0.00000000225938 $^\circ$ EC ^{2} SAR	0.9332	28.44
Fluvic Cambisol	$\overline{K}_{sat}$ = 0.02733608 + 0.000111962 *** EC − 0.0000000147655 *** EC ^{2} − 0.0024721 *** SAR	0.9306	25.66
Eutric Fluvisol	$\overline{K}_{sat}$ = 2.44341 + 0.000192643 *** EC − 0.0193937 *** SAR − 0.00000446051 ** EC SAR	0.8964	9.41

***, **, *, $^\circ$ 0.1%, 1%, 5%, and 10% of significance in *t*-test, respectively. [1] CV: coefficient of variation = (Standard deviation/Mean) × 100. [2] Transformed data by the equation $[X + 0.5]^{0.5}$—CV values collum.

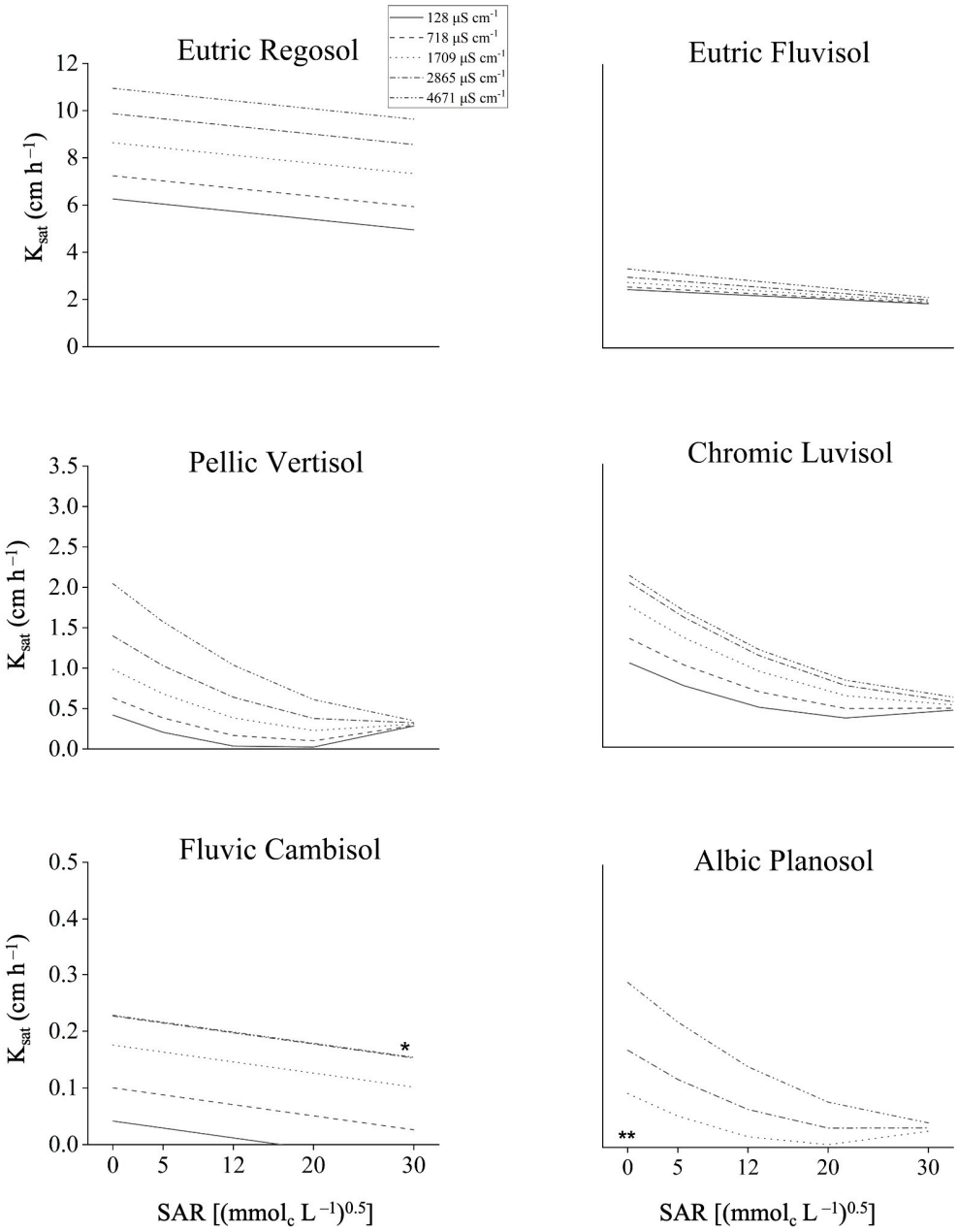

Figure 4. Saturated hydraulic conductivity (K_{sat}) of the soils as a function of the sodium adsorption ratio (SAR) for each EC_w of percolating water. Data obtained from multiple regression equations. Soils with different groups of scales depending on the speed of infiltration. * The lines referring to an EC_w of 2865 and 4671 µS cm^{-1} in Fluvic Cambisol are almost overlapped by the proximity of the estimated values by the equation. ** Lines referring to an EC_w of 128 and 718 µS cm^{-1} in Albic Planosol are overlapped with the x—axis.

The null K_{sat} (K_{sat0}) was estimated from the multiple regression equations, for each EC_w and SAR where the hydraulic conductivity is zero (Figure 5), matching the equations for K_{sat} = 0 to know at what level of EC_w and SAR the soil interrupts its drainage. In most soils, the SAR limit rose with the increase in electrical conductivity; however, Eutric Fluvisol showed a reverse behavior. The results show that the soils that easily achieve the null K_{sat} are Albic Planosol > Pellic Vertisol > Chromic Luvisol > Fluvic Cambisol > Eutric Fluvisol > Eutric Regosol. The first soil achieves the null K_{sat} (K_{sat0}) with the lowest Na^+ contents, and the last ones require higher Na^+ contents to modify the soil saturated hydraulic conductivity.

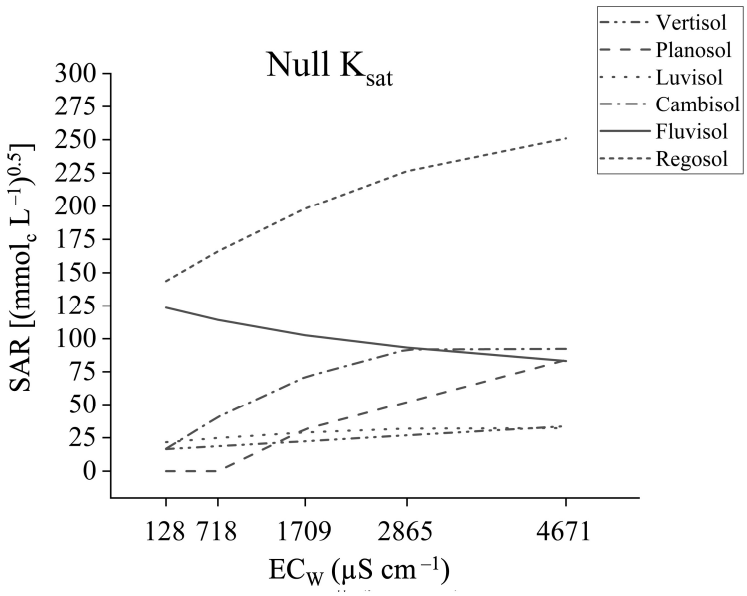

Figure 5. Null K_{sat}: values of sodium adsorption ratio (SAR), for each level of electrical conductivity (EC_w = 128, 817, 1709, 2865, and 4671 µS cm^{-1}), where the hydraulic conductivity of each soil is zero.

3.2. Threshold Electrolyte Concentration

We estimated the threshold electrolyte concentration (C_{TH}) of the soils evaluated to manage properly the soil–water system. The C_{TH} determines the values corresponding to the EC_w and the SAR of irrigation water where the K_{sat} is reduced by 20%, according to Ezlit et al. [1], indicating a significant dispersion of clay in the soil.

Figure 6 shows the threshold electrolyte concentration of the six soils that were reactive to saline waters. For all EC_w values established in this study, a SAR value is responsible for a 20% reduction of the maximum hydraulic conductivity, represented here as the relative hydraulic conductivity (rK_{sat}) of each soil. The SAR calculations were established from multiple regression equations developed for the six reactive soils.

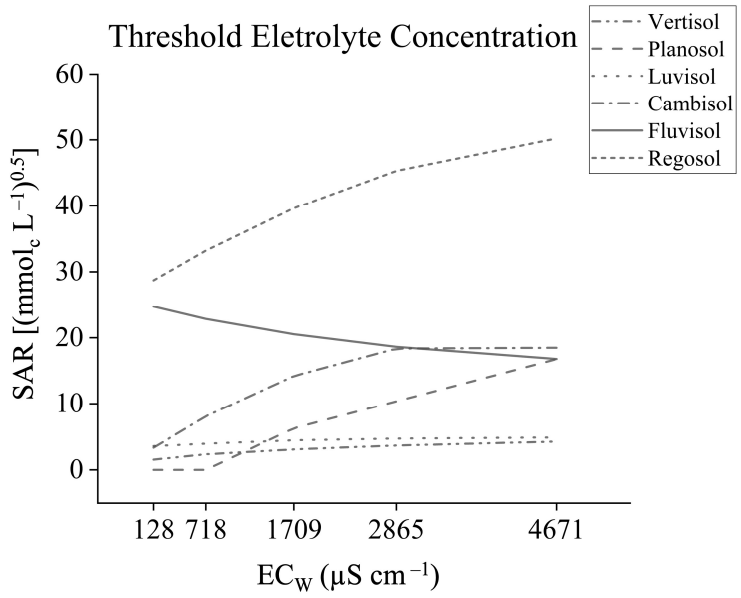

Figure 6. Threshold electrolyte concentration: SAR values, as a function of the EC_w, 128, 718, 1709, 2865, and 4671 µS cm^{-1}, representing a 20% reduction in the maximum hydraulic conductivity at each level of EC_w, for the reactive soils.

C_{TH} increased with the increment in EC_w, indicating that the higher the salt concentration, the more difficult it becomes to disperse soil colloids. Therefore, higher Na^+ contents are needed to promote dispersion in saline soil, due to its tendency to flocculate. The sequence of soils that easily achieve the C_{TH} was Albic Planosol > Pellic Vertisol > Chromic Luvisol > Fluvic Cambisol > Eutric Fluvisol > Eutric Regosol.

4. Discussion

4.1. Saturated Hydraulic Conductivity

Umbric Ferralsol, Haplic Lixisol, and Ferralic Nitisol soils are clayey and highly weathered, with an acidic pH, high exchangeable Al^{3+} (Table 3), high Fe concentration (Table 5), and a predominance of oxides and kaolinite in their clay mineralogy assemblage (Table 4). Therefore, stable aggregates are expected to form in these soils, indirectly verified by the high flocculation index, low bulk density, and high total porosity (Table 4). These properties allowed waters with distinct chemical qualities to pass without modification in the soil saturated hydraulic conductivity up to the limits established in this work (Figure 3 and Table 6) with an average K_{sat} of 2.75 cm h^{-1} for Ferralsol, 6.06 cm h^{-1} for Nitisol, and 3.33 cm h^{-1} for Lixisol.

For the pH values found in these three soils, there is an equilibrium of electrical charges in the clay fraction that allows for clay flocculation, corroborated by the high flocculation index (Table 4). This phenomenon is due to the isoelectric point (IEP) and point of zero charge (PZC), with both values related to the net surface charge [41,42]. Soil pH above the PZC shows a net negative charge, and soil below the PZC generates net positive charges. In the first case, the cation exchangeable capacity (CEC) will prevail, and in the latter case, the anion exchangeable capacity will prevail [43].

According to Kosmulski [42], for (hydr)oxides, such as goethite and hematite, their surface charge is controlled by two mechanisms: (1) protonation or deprotonation of surface oxygen atoms, and (2) leaching or adsorption of ion species from the (hydr)oxides into solution. As goethite and hematite have only pH-dependent surface charges and a high PZC varying from 7.0 to 9.0 [42,44], depending on the determination method, soils rich in these minerals, under acidic pH, favor the generation of positive charges.

However, the presence of organic matter and kaolinite, especially in highly weathered soils, usually tends to reduce the soil PZC, generating negative charges, which leads to an attraction of electrical charges among these colloids with (hydr)oxides [43,45]. Neutralization of soil charges results in stable aggregates that prevent changes in the K_{sat} of soils that have kaolinite and oxides as dominant minerals, independent of water quality (low or high ionic strength), as demonstrated in this study for Umbric Ferralsol, Haplic Lixisol, and Ferralic Nitisol soils (Figure 3).

Rand and Melton [46] detailed that the dynamics of clay in a soil solution are determined by the electrical double layers of two clay surfaces. According to the authors, the flocculation occurs in the lowest free energy of the system, when there is no potential energy to interfere with flocculation. However, when Na^+ is present in the soil solution at a high concentration, it causes the swelling of aluminosilicate in the clay fraction, which promotes dispersion, although Na^+ does not influence all soils at the same level [47].

Kaolinite is a clay mineral formed by one aluminum hydroxide octahedral sheet and one silica tetrahedral sheet. The small density of charges on the crystal basal surface is due to isomorphic substitution, but the pH-dependent surface charging is found at the edge hydroxyl groups due to broken bonds [45,46,48]. Due to the low isoelectric point (≈3–4) and isomorphic substitution of kaolinite, the charges in its minerals are negative even at soil low pH, which can lead to clay flocculation in soil rich in (hydr)oxides [43,46].

Despite the presence of smectite with a hydroxy-aluminum interlayer in the clay fraction, Haplic Lixisol had a similar trend as other weathered soils. The presence of smectite is uncommon for highly weathered soils, such as Lixisols. In these samples, it is possibly due to the soil parent material originating in the sedimentary basin of Cabo de Santo Agostinho (Pernambuco State, Brazil) from conglomerates with smectite in its composition, as described by Costa et al. [22]. The presence of a hydroxy-aluminum interlayer in smectite, due to the high Al^{3+} concentration in the soil, may explain the neutralization of negative charges of smectites. The presence of smectite is also corroborated by the greater clay activity in Haplic Lixisol (35.23 $cmol_c\ kg^{-1}$) than in Umbric Ferralsol (8.82 $cmol_c\ kg^{-1}$) and Ferralic Nitisol (23.69 $cmol_c\ kg^{-1}$). Freire et al. [39] observed a similar trend in the K_{sat} of two Lixisols from Pernambuco State (Northeast Brazil) under saline water, which are also highly weathered soils with a significant presence of oxides.

Tropical Brazilian soils, rich in iron and aluminum oxides, have a stronger aggregation that allow for a greater K_{sat} than soils from temperate climate even with a high clay concentration [49]. Generally, the presence of goethite, hematite, kaolinite, and gibbisite can be seen in the entire Brazilian territory [50], which indicates the presence of soils with high aggregation and satisfactory hydraulic conductivity properties. The presence of 2:1 minerals, such as smectite and illite, can be identified especially in arid and semiarid regions of the country, which can contribute to the reduction in the soil K_{sat}.

Sandier soils, such as Eutric Fluvisols and Eutric Regosols, were more reactive than highly weathered soils. Freire et al. [39] indicate that not only the texture but also the mineralogy assemblage of the soils was responsible for the different responses observed, similar to our study. Ottoni and collaborators [49] evaluated the natural K_{sat} of Brazilian soils from the north to south of the country. The authors compared K_{sat} data from some Brazilian research, and the result showed that sandy soils, such as Regosols, aways presented higher K_{sat} than clayey soils, such as Ferralsols, showing that the soil texture strongly influences soils' hydraulic properties.

The quality of the irrigation water influenced Eutric Regosol with a decrease in hydraulic conductivity at low EC_w and high SAR values (Figure 3). This soil has a pH value that is slightly higher than Umbric Ferralsol, Haplic Lixisol, and Ferralic Nitisol (Table 3), has low clay content, and has the lowest CEC (Table 3). Its flocculation index (FI) of only 29% (Table 4) can be associated with the presence of illite on the clay fraction (Table 4), in addition to the low content of Fe oxides (Table 5). This favors the dispersion process among colloids that move in the soil, clogging pores. Although Eutric Regosol is composed of 87.68% sand and only 2.82% clay (Table 4), the clay fraction is reactive to saline waters due to its illite-rich mineralogy (Table 4). Pedrón and coworkers [51], studying Regosols in Brazil, observed that the natural K_{sat} of the evaluated soils ranged from 0.00 to 6.40 cm h^{-1}, depending on the soil horizon, mineralogical assemblage, and soil texture. These differences in Regosols' composition interfere with the K_{sat} and can be aggravated depending on the quality of the water applied through irrigation, as shown in our present study.

The multiple regression equations (Table 6) showed that the greatest decreases in the estimated K_{sat} were in Pellic Vertisol, Chromic Luvisol, and Albic Planosol, due to the predominance of smectite. In these three soils, when waters of low ionic strength were applied, the K_{sat} became slow (K_{sat} < 0.5) for all SAR values. Although, when the salts levels increased, especially at an EC_w of 2865 and 4671 μS cm^{-1}, the higher Na^+ present in the system (SAR = 30), the lower the K_{sat} became. The opposite idea is, when we increased the Ca^{2+} concentration (SAR = 0), the K_{sat} became moderate (2.0 < K_{sat} < 6.25 cm h^{-1}) (Figure 4). For Pellic Vertisol at an EC_w of 4671 μS cm^{-1}, the K_{sat} ranged from moderate (2.04 cm h^{-1} in SAR 0) to slow (0.35 cm h^{-1} in SAR 30) (Figure 4). The same occurred in Chromic Luvisol at an EC_w of 2865 μS cm^{-1} (2.04 cm h^{-1} in SAR 0 and 0.56 cm h^{-1} in SAR

30). For Albic Planosol at an EC_w of 4671 µS cm^{-1}, the K_{sat} ranged from slow (0.29 cm h^{-1} in SAR 0) to very slow (0.04 cm h^{-1} in SAR 30).

Pellic Vertisol and Chromic Luvisol had very similar trends with the application of waters of different qualities. However, Chromic Luvisol had a higher K_{sat} than Pellic Vertisol in the most diluted waters (EC_w of 128 and 718 µS cm^{-1}) (Figure 4). This trend can be explained by the high proportion of Fe oxides, lower clay activity (AI = 61.75 $cmol_c$ kg^{-1}), and lower clay content (clay = 301.23 g kg^{-1}) in Chromic Luvisol (Tables 3–5) compared to Pellic Vertisol (AI = 75.44 $cmol_c$ kg^{-1}; clay = 424.98 g kg^{-1}), which leads to greater clay flocculation in Chromic Luvisol, raising the K_{sat}.

Furthermore, the clay fraction of Pellic Vertisol has a predominance of smectite, an expansive clay mineral with high reactivity to salts, while Chromic Luvisol has smectite, illite, kaolinite, and Fe (hydr) oxides (goethite and hematite). The assemblage of minerals in the Chromic Luvisol must have enabled a better flocculation index in this soil, because kaolinite and Fe oxides are less reactive to salts than smectite.

This study shows that soils with smectite in their mineralogical assemblage (e.g., Pellic Vertisol, Chromic Luvisol, Albic Planosol, and Eutric Fluvisol), respond to the ionic strength of applied waters differently in soils with only kaolinite and (hydr)oxides in their composition (e.g., Umbric Ferralsol and Ferralic Nitisol).

Smectite and kaolinite are phyllosilicate mineral species that differ from each other due to their structure. As mentioned before, kaolinite is considered a 1:1 mineral with one aluminum hydroxide octahedral sheet and one silica tetrahedral sheet [46,48]. Differently, smectite usually has an octahedral sheet (dioctahedral aluminum hydroxide or trioctahedral magnesium hydroxide) and two silica tetrahedral sheet linked by van der Waals forces, being considered a 2:1 mineral [52,53]. Due to the number of sheets and consequently high permanent charges (isomorphic substitution), smectites have a high cation exchange capacity (CEC), high clay activity, high specific surface area, and pH-dependent surface charges [47,54], which generate a greater net negative charge than others clay types.

Therefore, when we applied water with low ionic strength (EC_w of 128 and 718 µS cm^{-1}) in soils with the predominance of smectite and kaolinite, an excess of negative charges occurred, prevailing clay dispersion, pore obstruction, and consequently reducing K_{sat} (Figure 3). Conversely, when Ca^{+2} (divalent cation) was added to the system through water with a low SAR and high EC_w, the negative charges started to neutralize, allowing for flocculation and then raising the K_{sat}. On the other hand, in water with high ionic strength (EC_w of 2865 and 4671 µS cm^{-1}), but with a predominance of Na^+ (monovalent cation), a reduction in the K_{sat} also occurred due to the dynamics of the electrical double layers, which also lead to an excess of negative charges on the surfaces of smectites. So, smectites require exchangeable cations to balance their charges, especially divalent cations [53]. According to Jing and collaborators [55], the reduction in surface charge density with the addition of polarized ions such as K+ decreases the electrostatic repulsion (clay dispersion) and, consequently, increases the soil's hydraulic properties.

Despite the high level of sand (58%) and low level of clay (12%) (Table 4), Eutric Fluvisol was also affected by the treatments established in this work. In this soil, 53% of its granulometric composition is composed of fine sand (53%), while 29.88% is silt. Sand and silt particles are considered inert; nevertheless, they may be responsible for the obstruction of pores in the soil [56], making it difficult for water to pass through the soil and increasing the contact between salts and colloids. The clay fraction (12%) of this soil consists of smectite, illite, and kaolinite (Table 4). Again, the presence of smectite generates clay dispersion because it is an expansive mineral, and it has surplus electrical charges. Thus, illite, also an aluminosilicate, remains dispersed under high EC_w, due to its shape and low capability of cohesion [47]. In addition, the significant content of TOC (Table 3)

contributed to the generation of negative charges that react with the cations present in the applied treatments.

Fluvic Cambisol and Albic Planosol displayed the lowest K_{sat} values, with a significant response to the treatments applied (Figure 4). This is characteristic of soils with high activity in the clay fraction (AI > 27.00 $cmol_c\ kg^{-1}$); therefore, it is more reactive to waters with high salt levels. Eutric Cambisol and Albic Planosol have smectite, illite, and kaolinite in their mineralogy (Table 4) and an AI of 43.19 and 43.71 $cmol_c\ kg^{-1}$, respectively. The Albic Planosol had a higher clay concentration, and it showed a K_{sat} of zero (no drainage) when irrigated with water with a low EC_w and high SAR. With the application of percolating waters with an EC_w of 128 and 718 μS cm^{-1}, there was no drainage in Albic Planosol (Figure 4). The drainage only started at an EC_w of 1709 μS cm^{-1}, indicating that the excessive negative electrical charges, present mainly in the smectite minerals, began to be neutralized, allowing water to pass through soil column. This is evident at a higher EC_w, when the increase in the salt concentration, mainly Ca^{2+} (low SAR), raises the soil K_{sat} and possibly increases clay flocculation [57,58].

For Albic Planosol, the change in K_{sat} was from slow to very slow at an EC_w of 2865 μS cm^{-1} (0.17 cm h^{-1} in SAR 0 and 0.03 cm h^{-1} in SAR 30) and 4671 μS cm^{-1} (0.29 cm h^{-1} in SAR 0 and 0.04 cm h^{-1} in SAR 30) (Figure 4). Fluvic Cambisol showed a similar response with lower clay contents (23%) than Albic Planosol and a low K_{sat}, with a gradual increase, according to the increase in water salinity (Figure 3). However, the hydraulic conductivity of Fluvic Cambisol only reduces to zero at an EC_w of 128 μS cm^{-1} (Figure 4). This may be explained by the higher total sand proportion (42%) in Fluvic Cambisol (Table 4) as well as the higher Fe content (Table 5) and flocculation index (Table 4), compared to Albic Planosol.

Arora et al. [59] observed an increment in the soil hydraulic conductivity caused by saline waters due to greater soil aggregation and a greater flocculation index. Cucci et al. [60] reported a similar response in soils caused by the use of water with low, medium, and high concentrations of salts, indicating that small salt concentrations in the water reduce soil drainage. Our observations from the less evolved soils of the Brazilian tropical sub-humid and semiarid regions show that the K_{sat} of these soils (Regosol, Vertisol, Luvisol, Fluvisol, Cambisol, and Planosol) decreases with the reduction in the EC_w and the increase in the SAR in percolating waters. These data also corroborate the results of Yan et al. [61] who stated that a high EC_w can inhibit the influence of Na^+ on soil properties in irrigated areas.

This fact agrees with the Gouy-Chapman theory, which associates the influence of the ionic strength of the solution with the type and valence of the cations. High ionic concentrations in the solution and the valence of the cation reduce the thickness of the diffuse double layer, increasing clay flocculation.

On the other hand, increments in the SAR (Na^+ concentration in relation to Ca^{2+}) caused a decrease in the hydraulic conductivity at all EC levels of the six studied soils, revealing the Na^+-dispersing behavior. According to Yasin, Muhammend, and Mian [3], the increment in Na^+ in soils, without a proper leaching fraction, decreases their hydraulic conductivity, especially under a high exchangeable sodium percentage (ESP).

The K_{sat} was also low when water with a low electrolyte concentration (128 and 718 μS cm^{-1}), independent of the SAR, was applied to the soils that responded to the treatments. This occurs due to the low concentration of ions capable of neutralizing the excess charges of clay minerals, causing the total charge to remain negative and the clay particles to undergo repulsion. This can be attributed to the mineralogical assemblage of the soils, with the presence of 2:1-type clay minerals and a high negative charge density, especially for smectites and illites (Table 4). The influence of irrigation waters with increasing levels

of salts and Na^+ in soils with a high clay concentration and the presence of 2:1 minerals was reported by Ezlit et al. [1], Freire et al. [39], Chaudhari [62], Menezes et al. [63], Ali et al. [64], and Bennett et al. [65].

Although some chemical properties of the soil can be reverted, such as salinity and sodicity, others, once started, cannot be completely restored or reversed, such as the K_{sat} [66]. Centeno and coworkers [67] verified that soil management also decreases the soils' K_{sat}, where the K_{sat} of a native forest in the South of Brazil was 5.12 cm h^{-1} while areas with permanent cropping showed a K_{sat} of 1.30 cm h^{-1}. The same occurs in semiarid areas of Brazil, where the Ksat ranged from 5.3 cm h^{-1} in Luvisols with dense vegetation cover to 1.49 cm h^{-1} in Luvisol with sparse vegetation cover [68]. Therefore, appropriate water and soil management in areas at risk of degradation must be taken into consideration to avoid soil salinization/sodification.

The null K_{sat} calculation showed the differences among soils (Figure 5). The soils with the highest clay activity reached the null K_{sat0} quickly, indicating the strong influence of clay on water infiltration in the soil. Bennett et al. [65] reported similar results in Australian soils. The authors found that the reduction in the K_{sat} was directly related to the net negative charge of clay minerals and the proportion of clay present in the soils, where clayey soils are more reactive than less clayey soils.

In contrast, sandy soils, such as the Eutric Regosol soils, reach a null K_{sat0} at very high SAR levels (levels impossible to reach) due to the low content of clay minerals and organic matter and the high influence of the sand fraction on water percolation due to the predominance of macropores. Khataar et al. [69] reported that soil hydraulic conductivity depends mainly on the macropores, and their reduction or destruction reduces soil permeability. The authors state that sandy soils have greater hydraulic conductivity than clayey soils due to the predominance of pores with larger diameters.

Figure 5 shows the inversion in the null K_{sat} trend in the Eutric Fluvisol compared to the other soils. The high amount of TOC in Fluvisol (Table 3) is related to a high amount of organic matter (OM). Due to its composition, the OM reacts in saline/sodic soils in different ways [47]. Thus, one of the probable explanations for this inversion of Fluvisol concerning the null K_{sat} could be attributed to the influence of OM on charge generation and the affinity that its functional groups have with Ca^{2+} and Na^+, which can promote dispersion or flocculation of mineral components in the presence of salts. However, further studies on the types of charges in the OM and the visualization of the arrangement of mineral particles in Fluvisols are necessary to elucidate the inversion of the null K_{sat} trend observed in this type of soil.

In general, the use of water with increasing salt levels did not influence highly weathered soils with a significant presence of Fe (hydr) oxides and kaolinite. This indicates that irrigation does not affect the hydraulic conductivity of these soils up to the salinity/sodicity levels established in this work. However, water quality greatly affects soils from the semiarid regions with low weathering conditions and a greater presence of 2:1 clay minerals such as smectites and illites. This indicates a serious problem for the irrigated zones of the Brazilian semiarid region, a region that faces scarcity and poor distribution of rainfall during the year. According to Churchman et al. [47], the knowledge of soil clay mineralogy enables us to understand the effect that some cations, especially Na^+, have on soil permeability and how we can prevent or remedy the damage to physical attributes depending on the dynamics of these minerals.

The use of water with high levels of soluble salts is frequent in several irrigated zones in Brazil, resulting in the salinization and sodification of extensive areas [70]. According to saline and sodic water classification, ranging to C1 to C4 for salinity and S1 to S4 for sodicity [30], where C1 and C4 feature a low and high salt concentration, respectively,

waters classified as C3 and C4 (1709, 2865, and 4671 μS cm^{-1}), in this present work, ensure the soil's physical quality. On the other hand, C1 and C2 waters (128 and 718 μS cm^{-1}) reduced the soil saturated hydraulic conductivity, especially at a high SAR (waters classified as S3 and S4). Thus, studies on the chemical and physical properties are essential for each soil to adapt to the percolating waters.

Studies on the null K_{sat} are scarce. Therefore, research in the field is extremely necessary to reach adequate levels of salts in irrigation water for each soil type and each agricultural purpose. This can avoid chemical degradation due to the accumulation of salts and Na^+ as well as the physical degradation by soil densification and formation of impediment layers.

4.2. Threshold Electrolyte Concentration

Quirk and Schofield [71] developed the pioneering study on the threshold electrolyte concentration (C_{TH}). The researchers established that a reduction of 10 to 15% from the maximum K_{sat} indicates the critical onset of colloidal particle dispersion. However, recent studies show that this critical dispersion effect should be established at a 20% reduction from the maximum K_{sat} [1]. The C_{TH} increases with increasing EC_w (Figure 6), indicating that a high salt concentration in percolating waters favors colloids flocculation. Therefore, higher Na^+ contents are necessary to promote clay dispersion in saline soils.

In loamy soils with a predominance of 2:1 clay minerals, such as Pellic Vertisol, Albic Planosol, and Chromic Luvisol, the C_{TH} is reached more quickly, due to the high activity of the clays and the consequently high CEC (Table 3). In these soils, the clay dispersion features a greater Na^+ presence due to the predominance of negative charges. Therefore, water quality in these soils is even more crucial, preventing irrigation from causing soil degradation.

In sandier soils, such as Eutric Regosol and Fluvic Cambisol, with the EC_w increment, the C_{TH} is only reached at higher SAR values, mainly due to the presence of non-reactive particles, such as sand and silt, reducing the influence of Na^+ on the dispersion of colloidal particles and on the clogging of pores (Figure 6).

Eutric Fluvisol showed a different trend in C_{TH} compared with the other soils (Figure 6). The high TOC concentration in this soil (Table 3) possibly modified the electrochemical balance causing this reaction. However, further studies on soil natural organic matter dynamics in saline and sodic soils are necessary to understand the interaction between attraction and repulsion forces that act on flocculation and dispersion in these soils.

Some studies have highlighted the importance of evaluating C_{TH} for reducing the soil saturated hydraulic conductivity when Na^+ is added to the soil through irrigation water, mainly in soils with a significant presence of 2:1 minerals, such as smectites and vermiculites. The behavior observed in our study agrees with Menezes et al. [63], Bennett et al. [65], and Dang et al. [72].

The knowledge of C_{TH} is essential for the management of percolating waters in different soils. It can be useful to select adequate irrigation water by the balance among cations with flocculating and dispersing actions, such as Ca^{2+} and Na^+, respectively. In waters with a low EC_w and high SAR, the adjustment can be made with the addition of calcium via fertigation.

According to our data, for soils from tropical humid/hot climates, such as Ferrosols, Lixisols, and Nitisols, all rich in (hydr)oxides and kaolinite, the adjustment of the SAR does not change the soil K_{sat} up to the EC_w and SAR limits of this study. Therefore, the enhancement of Ca^{2+} in the soil solution, through the application of calcium amendments (e.g., $CaCO_3$ for soils with low pH or $CaSO_4$ for soils with high pH) applied to the soil or $CaNO_3$ or $CaCl_2$ applied as fertigation will only serve to provide Ca^{2+} for plant nutrition

demands and/or to increase soil pH, in the case of $CaCO_3$. However, for less weathered soils rich in 2:1 minerals, such as smectites and illites, the balance between Ca^{+2} and Na^+ is necessary to avoid soil physical degradation. In the case of less weathered soils, common in arid and semiarid areas, the application of calcium amendments can reduce soil degradation and improve agricultural use in areas where groundwater and drainage waters are high in sodium but are the only source of water for plants. Adjusting the Ca:Na ratio reduces the risk of sodicity and waterlogging in arid and semiarid soils [73] and provides Ca^{2+} for plant nutrition.

For Regosols, Cambisols, Fluvisols, Luvisols, Planosols, and Vertisols, the addition of Ca^{2+} amendments through the irrigation water needs to be conducted carefully (e.g., applying a reasonable leaching fraction) to avoid salinization. Monitoring water quality in arid and semiarid regions is essential to understand the dynamic of salts during the seasons. Also, the addition of calcium amendments ($CaSO_4$ applied to soil or $CaNO_3$ via fertigation) is useful in areas with sodic soils poor in Ca^{2+} and high in cations responsible for clay dispersion, such as Na^+ and Mg^{2+}. Thus, the equations shown in Table 6 can guide farmers to adjust their waters considering EC_w and SAR to simulate the effects of water quality in K_{sat}. The use of halophyte plants, such as quinoa (*Chenopodium quinoa* Willd.), atriplex (*Atriplex* spp.), and salicornia (*Salicornia* spp.), is also one strong strategy in areas where freshwater is not available for agriculture [74] and cation balancing through irrigation water is necessary to avoid soil degradation.

Thus, to maintain adequate soil-saturated hydraulic conductivity and good nutrition for plants, studies are needed to adjust the EC of waters with the required levels of macronutrients. This balanced management, based on the physical–chemical characteristics of the water and soil, allows for satisfactory physical and chemical qualities of the soil without promoting its degradation by the accumulation of salts and Na^+ and by densification caused by the dispersion of colloids. Nevertheless, further studies on C_{TH} are necessary.

5. Conclusions

This study showed that the ionic composition of irrigation water affected the water percolation of six soils representing tropical sub-humid and semiarid climates but not the three soils from a tropical humid climate. Water percolation in the soil, measured through its saturated hydraulic conductivity (K_{sat}), varied according to clay type and concentration, where soils with smectites and illites were more prone to degradation than soils rich in (hydr)oxides and kaolinites. The determination of the threshold electrolyte concentration (C_{TH}) showed that soil physical degradation will occur faster in clayey soils rich in high-activity clays when irrigated with highly sodic waters, and that sandy soils are less susceptible to physical degradation when irrigated with the same type of water. Under non-saline and saline waters (e.g., 128 and 4671 $\mu S\ cm^{-1}$), the C_{TH} of sandy soils such as Eutric Regosol was reached under a SAR 30- to 50-fold higher than in clayey soils rich in smectites, such as Albic Planosol and Pellic Vertisol, which proves the high susceptibility of clayey soils, rich in smectites and illites, to soil physical degradation. Also, regardless of water salinity (EC_w), the six types of tropical sub-humid and semiarid soils tested here proved to be more prone to soil physical degradation if the waters were rich in Na^+ than if they were rich in Ca^{2+}. Thus, the determination of the C_{TH} in soils will allow farmers to establish the best irrigation management practice to avoid physical degradation and soil salinization/sodification, especially in arid and semiarid regions. The null K_{sat} followed the same trend as the C_{TH}, showing that soil drainage can be more easily interrupted in clayey soil rich in smectites than in sandy soils, proving that waters with a SAR lower than 25 can completely degrade the hydraulic properties of soils from tropical sub-humid and semiarid climates. Water ionic composition affected primarily tropical sub-humid and semiarid soils,

such as Pellic Vertisol, Albic Planosol, Chromic Luvisol, and Fluvic Cambisol. However, the water percolation in tropical humid soils, such as Umbric Ferralsol, Ferralic Nitisol, and Haplic Lixisol was not affected by the ionic composition of the waters evaluated in this study. Also, when faced with waters that are high in Na^+ and/or poor in Ca^{2+}, farmers can delay or mitigate soil sodification by adding calcium amendments directly to the soil or through the fertigation water. This research shows the importance of knowing the interaction between soil type and irrigation water composition to implement management practices aimed at preventing the chemical and physical degradation of agricultural soils. Further studies should focus on good management practices related to irrigation water use and fertigation to increase crop productivity, soil conservation, and soil preservation.

Supplementary Materials: The following supporting information can be downloaded at https://www.mdpi.com/article/10.3390/agronomy15040864/s1: Figure S1: Mineralogy of clay fraction determined by x-ray diffractometry. Fd—feldspar; K—kaolinite; S—smectite; I—illite; HIS—smectite with hydroxy-aluminum interlayer; and Tc—talc.

Author Contributions: Conceptualization: C.B.V. and M.B.G.d.S.F.; Investigation: C.B.V., G.H.M.C.S., B.G.d.A., F.J.F., V.S.d.S.J., L.G.M.P., H.F.d.M. and M.B.G.d.S.F.; Methodology: C.B.V., G.H.M.C.S., L.G.G.d.L., R.F.d.N.P. and M.B.G.d.S.F.; Project administration: C.B.V. and M.B.G.d.S.F.; Formal analysis: C.B.V., G.H.M.C.S., L.G.G.d.L. and R.F.d.N.P.; Data curation: C.B.V., M.B.G.d.S.F., F.J.F., V.S.d.S.J. and B.G.d.A.; Resources: M.B.G.d.S.F.; Supervision: M.B.G.d.S.F.; Validation: C.B.V.; Visualization: C.B.V. and M.B.G.d.S.F.; Writing—original draft: C.B.V., G.H.M.C.S., M.B.G.d.S.F. and J.F.d.S.F.; Writing—review and editing: C.B.V., M.B.G.d.S.F., G.H.M.C.S., L.G.M.P., B.G.d.A., V.S.d.S.J. and J.F.d.S.F. All authors have read and agreed to the published version of the manuscript.

Funding: This research received no external funding.

Data Availability Statement: Data are available from the corresponding author upon reasonable request.

Acknowledgments: This work was financially supported by the Foundation of Support to Science and Technology of Pernambuco (FACEPE) under Grant number 0661-5.01/17, the National Council for Scientific and Technological Development (CNPq), and the Coordination for the Improvement of Higher Education Personnel (CAPES). We are grateful for the support of the Federal Rural University of Pernambuco and the soil science group of this institution.

Conflicts of Interest: The authors declare no conflicts of interest.

References

1. Ezlit, Y.D.; Bennett, L.M.; Raine, S.R.; Smith, R.J. Modification of the McNeal Clay Swelling Model Improves Prediction of Saturated Hydraulic Conductivity as a Function of Applied Water Quality. *Soil Sci. Soc. Am. J.* **2013**, *77*, 2149–2156. [CrossRef]
2. Mohanavelu, A.; Naganna, S.R.; Al-Ansari, N. Irrigation Induced Salinity and Sodicity Hazards on Soil and Groundwater: An Overview of Its Causes, Impacts and Mitigation Strategies. *Agriculture* **2021**, *11*, 983. [CrossRef]
3. Yasin, M.; Muhammed, S.; Mian, S.M. Hydraulic conductivity and ESP of soils affected by sodic water. *Pakistan J. Agric. Res.* **1989**, *10*, 289–294.
4. Singh, A. Soil salinization management for sustainable development: A review. *J. Environ. Manag.* **2021**, *277*, 111383. [CrossRef] [PubMed]
5. Usowicz, B.; Lipiec, J. Spatial variability of saturated hydraulic conductivity and its links with other soil properties at the regional scale. *Sci. Rep.* **2021**, *11*, 8293. [CrossRef]
6. Yao, R.; Yang, J.; Wu, D.; Li, F.; Gao, P.; Wang, X. Evaluation of pedotransfer functions for estimating saturated hydraulic conductivity in coastal salt-affected mud farmland. *J. Soils Sediments* **2015**, *15*, 902–916. [CrossRef]
7. Blanco-Canqui, H.; Wienhold, B.; Jin, V.; Schmer, M.; Kibet, L. Long-term tillage impact on soil hydraulic properties. *Soil Till. Res.* **2017**, *170*, 38–42. [CrossRef]
8. Souza, L.S.; Mafra, A.L.; Souza, L.D.; Silva, I.F.; Klein, V.A. Inter-relação entre manejo e atributos físicos. In *Manejo e Conservação do Solo e da água*, 1st ed.; Bertol, I., De Maria, I.C., Souza, L.S., Eds.; SBCS: Viçosa, Brazil, 2019; Volume 1, pp. 193–249.
9. Zhu, Y.; Bennett, J.M.; Marchuk, A. Reduction of hydraulic conductivity and loss of organic carbon in non-dispersive soils of different clay mineralogy is related to magnesium induced disaggregation. *Geoderma* **2019**, *349*, 1–10. [CrossRef]

10. Quirk, J.P. Chemistry of saline soils and their physical properties. In *Salinity and Water Use*; Part II; Talsma, T., Philip, J.R., Eds.; Palgrave Macmillan: London, UK, 1971; pp. 79–91.
11. Qadir, M.; Ghafoor, A.; Murtaza, G. Amelioration strategies for saline soils: A review. *Land Degrad. Dev.* **2000**, *11*, 501–521. [CrossRef]
12. Demattê, J.A.M.; Dotto, A.C.; Paiva, A.F.S.; Sato, M.V.; Dalmolin, R.S.D.; Araújo, M.S.B.; Silva, E.B.; Nanni, M.R.; ten Caten, A.; Noronha, N.C.; et al. The Brazilian Soil Spectral Library (BSSL): A general view, application and challenges. *Geoderma* **2019**, *354*, 113793. [CrossRef]
13. Alvares, C.A.; Stape, J.L.; Sentelhas, P.C.; Gonçalves, J.L.M.; Sparovek, G. Köppen's climate classification map for Brazil. *Meteorol. Z.* **2013**, *22*, 711–728. [CrossRef] [PubMed]
14. Brasil. Centro Nacional de Monitoramento e Alertas de Desastres Naturais. Estudo do CEMADEN e do INPE Identifica pela Primeira vez a Ocorrência de uma Região árida no país. Available online: https://www.gov.br/cemaden/pt-br/assuntos/noticias-cemaden/estudo-do-cemaden-e-do-inpe-identifica-pela-primeira-vez-a-ocorrencia-de-uma-regiao-arida-no-pais (accessed on 20 February 2025).
15. Santos, H.G.; Jacomine, P.K.T.; Anjos, L.H.C.; Oliveira, V.A.; Lumbreras, J.F.; Coelho, M.R.; de Almeida, J.A.; de Araujo Filho, J.C.; Oliveira, J.B.; Cunha, T.J.F. *Brazilian Soil Classification System*; Embrapa: Brasília, Brazil, 2018; p. 353.
16. Souza, J.L.L.; Castro, F.E.; Andadre, C.V.P.A.; Ker, J.C.; Perez Filho, A. Brazilian semiarid soils formed during the last glacial maximum. *Catena* **2023**, *233*, 106899. [CrossRef]
17. Pessoa, L.G.M.; Freire, M.B.G.S.; Wilcox, B.P.; Green, C.H.M.; Araújo, R.J.T.; Araújo Filho, J.C. Spectral reflectance characteristics of soils in northeastern Brazil as influenced by salinity levels. *Environ. Monit. Assess.* **2016**, *188*, 616. [CrossRef] [PubMed]
18. Santos, J.C.B.; Souza Júnior, V.S.; Corrêa, M.M.; Ribeiro, M.R.; Almeida, M.C.; Borges, L.E.P. Caracterização de Neossolos Regolíticos da região semiárida do estado de Pernambuco. *Rev. Bras. Cienc. Solo* **2012**, *36*, 683–695. [CrossRef]
19. Lima, G.K. Caracterização de Vertissolos do Nordeste Brasileiro. Master's Dissertation, Federal Rural University of Pernambuco, Recife, Brazil, 2014.
20. Santana, M.B. Caracterização e Classificação de Solos na Ilha de Assunção, Cabrobó–Pernambuco. Ph.D. Dissertation, Federal Rural University of Pernambuco, Recife, Brazil, 2015.
21. Araújo, J.K.S.; Souza Júnior, V.S.; Marques, F.A.; Voroney, P.; Souza, R.A.S.; Corrêa, M.M.; Câmara, E.R.G. Umbric Ferralsols along a climosequence from the Atlantic coast to the highlands of northeastern Brasil: Characterization and carbon mineralization. *Geoderma* **2017**, *293*, 34–43. [CrossRef]
22. Costa, E.U.C.; Santos, J.C.B.; Azevedo, A.C.; Araújo Filho, J.C.; Corrêa, M.M.; Neves, L.V.M.W.; Vidal-Torrado, P.; Souza-Júnior, V.S. Mineral alteration and genesis of Al–rich soils derived from conglomerate deposits in Cabo Basin, NE Brazil. *Catena* **2018**, *167*, 198–211. [CrossRef]
23. Neves, L.V.M.W.; Santos, J.C.B.; Souza Júnior, V.S.; Corrêa, M.M.; Araújo Filho, J.C. Associations between attributes of Nitisols and the climate of the southern coast of Pernambuco. *Rev. Caatinga* **2018**, *31*, 255–263. [CrossRef]
24. Sousa, J.E.S.; Santos, J.C.B.; Corrêa, M.M.; Nascimento, A.F.; Schulze, S.M.B.B.; Ferreira, T.O.; Araújo Filho, J.C.; Souza Júnior, V.S. Mineralogy and genesis of Planosols under a semi-arid climate, Borborema Plateau, NE Brazil. *Catena* **2020**, *184*, 104260. [CrossRef]
25. Sousa, M.G.; Araujo, J.K.S.; Ferreira, T.O.; Andrade, G.R.P.; Araújo Filho, J.C.; Fracetto, G.G.M.; Santos, J.C.B.; Fracetto, F.J.C.; Lima, G.K.; Souza Junior, V.S. Long-term effects of irrigated agriculture on Luvisol pedogenesis in semi-arid region, northeastern Brazil. *Catena* **2021**, *206*, 105529. [CrossRef]
26. Governo do Estado de Pernambuco. Atlas Eólico e Solar de Pernambuco. Available online: http://www.atlaseolicosolar.pe.gov.br/ (accessed on 20 February 2025).
27. IUSS Working Group WRB. *World Reference Base for Soil Resources. International Soil Classification System for Naming Soils and Creating Legends for Soil Maps*, 4th ed.; International Union of Soil Sciences (IUSS): Vienna, Austria, 2022; p. 236.
28. Yeomans, J.C.; Bremner, J.M. A rapid and precise method for routine determination of organic carbon in soil. *Commun. Soil Sci. Plant Anal.* **1988**, *19*, 1467–1476. [CrossRef]
29. Teixeira, P.C.; Donagemma, G.K.; Fontana, A.; Teixeira, W.G. *Manual de Métodos de Análise de Solo*, 3rd ed.; Embrapa: Brasília, Brazil, 2017; p. 574.
30. Richards, L.A. *Diagnosis and Improvement of Saline and Alkali Soils*; US Department of Agriculture: Washington DC, USA, 1954; Volume 78, p. 166.
31. Gee, G.W.; Or, D. Particle Size Analysis. In *Methods of Soil Analysis, Part 4, Physical Methods*, 1st ed.; Dane, J.H., Topp, G.C., Eds.; Book Series No. 5; Soils Science Society of America: Madison, WI, USA, 2002; pp. 255–293.
32. International Organization for Standardization (ISO). *Soil Quality-Determination of Dry Bulk Density*; International Organization for Standardization: Geneva, Switzerland, 2017.
33. Flint, A.L.; Flint, L.E. Particle density. In *Methods of Soil Analysis, Part 4, Physical Methods*, 1st ed.; Dane, J.H., Topp, G.C., Eds.; Book Series, 5; Soils Science Society of America: Madison, WI, USA, 2002; pp. 255–293.

34. Kiehl, E.J. *Manual de Edafologia: Relações Solo-Planta*; Agronômica Ceres: São Paulo, Brazil, 1979; p. 263.
35. Mehra, O.P.; Jackson, M.L. Iron oxide removal from soils and clays by a dithionite-citrate system buffered with sodium bicarbonate. *Clays Clay Miner.* **1958**, *7*, 317–327. [CrossRef]
36. Jackson, M.L. *Soil chemical analysis: Advanced Course: A Manual of Methods Useful for Instruction and Research in Soil Chemistry, Physical Chemistry of Soils, Soil Fertility, and Soil Genesis*; Madison Libraries: Madison, WI, USA, 1975; p. 930.
37. Brown, G.; Brindley, G.W. X-ray Diffraction Procedures for clay mineral identification. In *Crystal Structures of Clays Minerals and Their X-ray Identification*, 1st ed.; Brindley, G.W., Brown, G., Eds.; Mineralogical Society: London, UK, 1980; pp. 305–356.
38. Moore, D.M.; Reynolds, R.C. *X-Ray Diffraction and Identification and Analysis of CLAY Minerals*; Oxford University Press: Oxford, UK, 1989; p. 332.
39. Freire, M.B.G.S.; Ruiz, H.A.; Ribeiro, M.R.; Ferreira, P.A.; Alvarez, V.H.; Freire, F.J. Condutividade hidráulica de solos de Pernambuco em resposta à condutividade elétrica e RAS da água de irrigação. *Rev. Bras. Eng. Agric. Ambient.* **2003**, *7*, 45–52. [CrossRef]
40. Klute, A. Laboratory measurement of hydraulic conductivity of saturated soil. In *Methods of Soil Analysis, Part 1*, 1st ed.; Black, C.A., Ed.; American Society of Agronomy: Madison, WI, USA, 1965; pp. 210–221.
41. Parks, G. The isoelectric points of solid oxides, solid hydroxides, and aqueous hydroxo complex systems. *Chem. Rev.* **1965**, *65*, 177–198. [CrossRef]
42. Kosmulski, M. Isoelectric points and points of zero charge of metal (hydr)oxides: 50 years after Parks' review. *Adv. Colloid Interface Sci.* **2016**, *238*, 1–61. [CrossRef] [PubMed]
43. Appel, C.; Ma, L.Q.; Rhue, R.D.; Kennelley, E. Point of zero charge determination in soils and minerals via traditional methods and detection of electroacoustic mobility. *Geoderma* **2003**, *113*, 77–93. [CrossRef]
44. Parks, G.A.; Bruyn, P.L. The zero point of charge of oxides. *J. Phys. Chem.* **1962**, *66*, 967–973. [CrossRef]
45. Schofield, R.K.; Samson, H.R. Flocculation of kaolinite due to the attraction of oppositely charged crystal faces. *Disc. Faraday Soc.* **1954**, *18*, 135–145. [CrossRef]
46. Rand, B.; Melton, I. Isoelectric point of the edge surface of kaolinite. *Nature* **1975**, *257*, 214–216. [CrossRef]
47. Churchman, G.J.; Skjemstad, J.O.; Oades, J.M. Influence of clay minerals and organic matter on effects of sodicity on soils. *Aust. J. Soil Res.* **1993**, *31*, 779–800. [CrossRef]
48. Mbey, J.A.; Thomas, F.; Razafitianamaharavo, A.; Caillet, C.; Villiéras, F. A comparative study of some kaolinites surface properties. *Appl. Clay Sci.* **2019**, *172*, 135–145. [CrossRef]
49. Ottoni, M.V.; Teixeira, W.G.; Reis, A.M.H.; Pimentel, L.G.; Souza, L.R.; Albuquerque, J.A.; Melo, V.F.; Cavalieri-Polizeli, K.M.V.; Reichert, J.M.; Viana, J.H.M.; et al. Saturated hydraulic conductivity and steady-state infiltration rate database for Brazilian soils. *Rev. Bras. Cienc. Solo.* **2025**, *49*, e0240003. [CrossRef]
50. Rosin, N.A.; Demattê, J.A.M.; Poppiel, R.R.; Silvero, N.E.Q.; Rodriguez-Albarracin, H.S.; Rosas, J.T.F.; Greschuk, L.T.; Bellinaso, H.; Minasny, B.; Gomez, C.; et al. Mapping Brazilian soil mineralogy using proximal and remote sensing data. *Geoderma* **2023**, *432*, 116413. [CrossRef]
51. Pedron, F.A.; Deobald, G.A.; Gubiani, P.I.; Santos, L.A.C.; Azevedo, A.C.; Reichert, J.M.; Dambroz, A.P.B. Soil hydraulic properties, mineralogical alteration and pore formation in Regosols from southern Brazil. *Rev. Bras. Cienc. Solo.* **2024**, *48*, e0240013. [CrossRef]
52. Thomas, F.; Michot, L.J.; Vantelon, D.; Montargès, E.; Prélot, B.; Cruchaudet, M.; Delon, J.F. Layer charge and electrophoretic mobility of smectites. *Colloids Surf. A Physicochem. Eng. Asp.* **1999**, *159*, 351–358. [CrossRef]
53. Morris, G.E.; Zbik, M.S. Smectite suspension structural behaviour. *Int. J. Miner. Process* **2009**, *93*, 20–25. [CrossRef]
54. Kaufhold, S.; Dohrmann, R. The variable charge of dioctahedral smectites. *J. Colloid Interface Sci.* **2013**, *390*, 225–233. [CrossRef]
55. Jing, Y.; Ding, W.; Liu, X. Saturated hydraulic conductivities in saline-alkali soil dependent on electrostatic repulsion between particles considering polarization effects. *J. Soils Sediments* **2025**, 1–11. [CrossRef]
56. Fetzer, J.; Holzner, M.; Plötzer, M.; Furrer, G. Clogging of an Alpine streambed by silt-sized particles e Insights from laboratory and field experiments. *Water Res.* **2017**, *126*, 60–69. [CrossRef]
57. Hussain, N.; Hassan, G.; Arshadullah, M.; Mujeeb, F. Evaluation of Amendments for the Improvement of Physical Properties of Sodic Soil. *Int. J. Agric. Biol.* **2001**, *3*, 319–322.
58. Vasconcelos, R.R.A.; Barros, M.F.C.; Silva, E.F.F.; Graciano, E.S.A.; Fontenele, A.J.P.B.; Silva, N.M.L. Características físicas de solos salino-sódicos do semiárido pernambucano em função de diferentes níveis de gesso. *Rev. Bras. Eng. Agric. Ambient.* **2013**, *17*, 1318–1325. [CrossRef]
59. Arora, N.K.; Chaudhari, S.K.; Yadav, R.K.; Sharma, P.C. Saturated hydraulic conductivity, dispersion index and water retention changes in salt affected soils under different quality water irrigation. *J. Soil Salin. Water Qual.* **2019**, *11*, 1–9.
60. Cucci, G.; Lacolla, G.; Rubino, P. Irrigation with saline-sodic water: Effects on soil chemical-physical properties. *Afr. J. Agric. Res.* **2013**, *8*, 358–365. [CrossRef]
61. Yan, S.; Zhang, T.; Zhang, B.; Feng, H. A revised saline water quality assessment method considering including Mg2+/Na+ as a new indicator for an arid irrigated area. *J. Hydrol.* **2024**, *639*, 131619. [CrossRef]

62. Chaudhari, S.K. Saturated hydraulic conductivity, dispersion, swelling, and exchangeable sodium percentage of different textured soils as influenced by water quality. *Commun. Soil Sci. Plant Anal.* **2001**, *32*, 2439–2455. [CrossRef]
63. Menezes, H.R.; Almeida, B.G.; Almeida, C.D.G.C.; Bennett, J.M.; Silva, E.M.; Freire, M.B.G.S. Use of threshold electrolyte concentration analysis to determine salinity and sodicity limit of irrigation water. *Rev. Bras. Eng. Agric. Ambient.* **2014**, *18*, 53–58. [CrossRef]
64. Ali, A.; Biggs, A.J.W.; Marchuk, A.; Bennett, J.M. Effect of irrigation water pH on saturated hydraulic conductivity and electrokinetic properties of acidic, neutral, and alkaline soils. *Soil Sci. Soc. Am. J.* **2019**, *83*, 1671–1681. [CrossRef]
65. Bennett, J.M.; Marchuk, A.; Marchuk, S.; Raine, S.R. Towards predicting the soil-specific threshold electrolyte concentration of soil as a reduction in saturated hydraulic conductivity: The role of clay net negative charge. *Geoderma* **2019**, *337*, 122–131. [CrossRef]
66. Adeyemo, T.; Kramer, I.; Levy, G.J.; Mau, Y. Salinity and sodicity can cause hystereses in soil hydraulic conductivity. *Geoderma* **2022**, *413*, 115765. [CrossRef]
67. Centeno, L.N.; Timm, L.C.; Reichardt, K.; Beskow, S.; Caldeira, T.L.; Oliveira, L.M.; Wendroth, O. Identifying regionalized co-variate driving factors to assess spatial distributions of saturated soil hydraulic conductivity using multivariate and state-space analyses. *Catena* **2020**, *191*, 104583. [CrossRef]
68. Lins, C.M.T.; Souza, E.R.; Souza, T.E.M.S.; Paulino, M.K.S.S.; Monteiro, D.R.; Souza Júnior, V.S.; Dourado, P.R.M.; Rego Junior, F.E.A.; Silva, Y.J.A.; Schaffer, B. Influence of vegetation cover and rainfall intensity on soil attributes in an area undergoing desertification in Brazil. *Catena* **2023**, *221*, 106751. [CrossRef]
69. Khataar, M.; Mosaddeghi, M.R.; ·Chayjan, R.A.; Mahboubi, A.A. Prediction of water quality effect on saturated hydraulic conductivity of soil by artificial neural networks. *Paddy Water Environ.* **2018**, *16*, 631–641. [CrossRef]
70. Pessoa, L.G.M.; Freire, M.B.G.S.; Santos, R.L.; Freire, F.J.; Miranda, M.F.A.; Santos, P.R. Saline water irrigation in semiarid region: I—effects on soil chemical properties. *Aust. J. Croup Sci.* **2019**, *13*, 1169–1176. [CrossRef]
71. Quirk, J.P.; Schofield, R.K. The effect of electrolyte concentration on soil permeability. *Aust. J. Soil Res.* **1955**, *6*, 163–178. [CrossRef]
72. Dang, A.; Bennett, J.M.; Marchuk, A.; Biggs, A.; Raine, R.S. Quantifying the aggregation-dispersion boundary condition in terms of saturated hydraulic conductivity reduction and the threshold electrolyte concentration. *Agric. Water Manag.* **2018**, *203*, 172–178. [CrossRef]
73. Rengasamy, P. Importance of calcium in irrigation with saline-sodic water—A viewpoint. *Agric. Water Manag.* **1987**, *12*, 207–219. [CrossRef]
74. Hasnain, M.; Abideen, Z.; Ali, F.; Hasanuzzaman, M.; El-Keblawy, A. Potential of Halophytes as Sustainable Fodder Production by Using Saline Resources: A Review of Current Knowledge and Future Directions. *Agronomy* **2023**, *12*, 2150. [CrossRef]